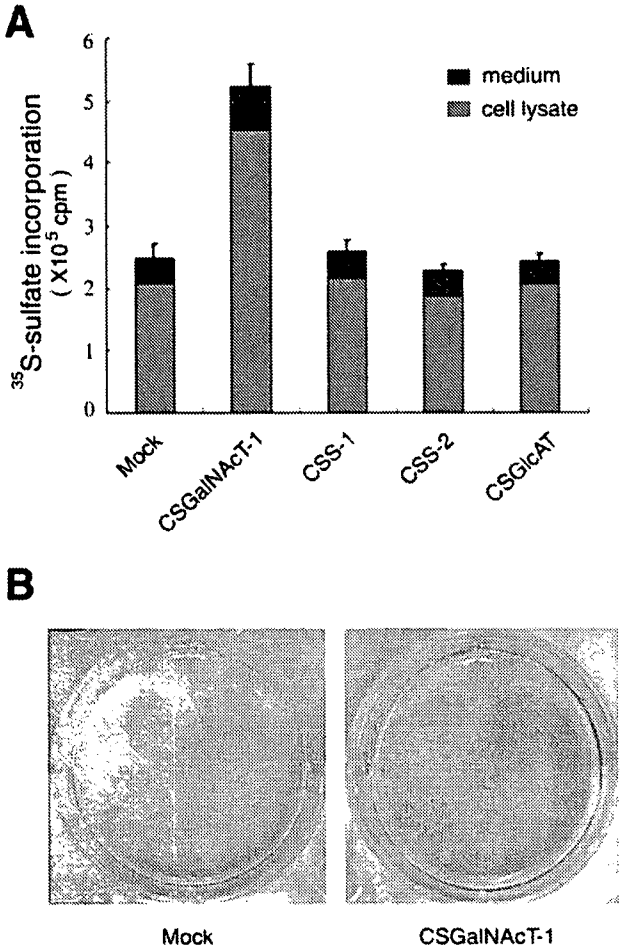

FIGURE 5. **Increased CS levels following the overexpression of CSGalNAcT-1 in LTC cells.** Stable transfectants overexpressing CSGalNAcT-1, CSS-1, CSS-2, CSGlcAT, and mock transfectants were established by transfecting LTC cells with expression vectors of the enzyme genes followed by selection with G418 for 10 days. *A*, [^{35}S]sulfate incorporation of mock-transfected cells and CSGalNAcT-1-, CSS-1-, CSS-2-, and CSGlcAT-overexpressing cells is shown (*gray bar*, cell lysates; *black bar*, conditioned medium). Note that CSGalNAcT-1-overexpressing cells exhibit an ~2.2-fold increase in CS biosynthesis compared with the mock-transfected cells, whereas the others do not. *B*, culture plates stained with Alcian blue (pH 1.0). CSGalNAcT-1-overexpressing cells exhibited a stronger staining intensity than the mock-transfected cells.

ugation followed by dot blot detection of aggrecan core protein showed that aggrecan obtained from the CSGalNAcT-1-overexpressing cells was present in the bottom fractions, whereas aggrecan from the mock-transfected cells was widely distributed (Fig. 6*C*). Immunohistochemically, CS stained stronger in the pericellular zone of the CSGalNAcT-1-overexpressing cells than in the mock-transfected cells, whereas aggrecan core protein stained at similar levels (Fig. 6*D*). These observations indicate that aggrecan in the CSGalNAcT-1-overexpressing cells contains a larger amount of CS.

The increased amounts of CS imply that there is an increased number of CS chains or greater elongation of individual CS chains in GSGalNAcT-1-transfected cells. To examine CS chain length, we performed metabolic labeling of the CS chains synthesized in the transfected cells and subjected them to gel chromatography. The elution profile demonstrated CS chains with peaks at the same position (Fig. 7*A*, *arrows*). Furthermore, direct molecular sieve analysis of ^{3}H-labeled CS chains confirmed the same size of CS chains (Fig. 7*B*). These results indicate that the CS chain length in GSGalNAcT-1 and mock-transfected cells was similar, although there was an ~2.2-fold increase in CS incorporation in the CSGalNAcT-1-overexpressing cells. The functions of the CS chains, such as water absorption, depend on their saccharide structure, including sulfation (36). When the CS disaccharide composition was analyzed, a similar ratio of hexuronic acid (HexA)-GalNAc, HexA-GalNAc(4S), and the other disaccharides was observed in both the GSGalNAcT-1- and mock-transfected cells (9.9, 88.2, and 1.9% for mock; 4.3, 93.6, and 2.1% for CSGalNAcT-1-overexpressing cells) (Fig. 7*C*). Therefore, CSGalNAcT-1 overexpression appeared to cause a 2.2-fold increase in the number of CS chains along with a similar sulfation level per chain.

In Vivo Gene Delivery of CSGalNAcT-1 Increases CS Biosynthesis in Cartilage—Our *in vitro* studies using cell lines demonstrated that CSGalNAcT-1 overexpression increases CS biosynthesis. Since chondrocytes *in vivo* may utilize a similar mechanism, we tested whether *in vivo* gene delivery of CSGalNAcT-1 increases CS biosynthesis in cartilage. A replication-deficient adenovirus 5 containing a cDNA encoding CSGalNAcT-1 and the V5 epitope tag was injected into the nucleus pulposus of the intervertebral discs of 4-month-old mice, and its expression was confirmed by immunostaining for the V5 tag (data not shown). Histological analysis at day 7 after the injection showed intense Alcian blue staining in the pericellular zone of the nucleus pulposus cells in the disc and chondrocytes in the vertebral endplate compared with mice injected with the control adenovirus (Fig. 8). These results demonstrated that *in vivo* gene delivery of CSGalNAcT-1 in fact increased CS biosynthesis in cartilage.

DISCUSSION

In this study, we identified CSGalNAcT-1 as a key enzyme for CS biosynthesis in cartilage. Analysis of the expression patterns of glycosyltransferases and aggrecan core protein in normal developing cartilage by *in situ* hybridization, in chondrogenic cell lines, and in the aggrecan-null cartilage of cmd mice demonstrated both high level expression of CSGalNAcT-1 and good correlation of its expression with that of aggrecan core protein. Furthermore, CSGalNAcT-1 overexpression in cultured chondrocytic cells and the intervertebral disc elevated CS synthesis in the cells. These observations suggest that CSGalNAcT-1 is still unsaturated in chondrocytes, and an increase in the level of CS via its overexpression leads to prevention of cartilage destruction.

Of the six glycosyltransferases involved in CS biosynthesis, CSGalNAcT-1 expression was the highest in E18.5 mouse cartilage exhibiting ~170-fold higher expression than that of CSGalNAcT-2 (Fig. 4*B*). In tissues other than cartilage, CSGalNacT-1 is expressed at the highest level in the thyroid gland and placenta, which exhibit expression only up to 1.5–5-fold that of CSGalNAcT-2 (20). In addition, various cell lines show relatively low levels of CSGalNAcT-1 expression compared with other enzymes (18).[3] Thus, the high expression of CSGalNAcT-1 appears to be characteristic of chondrocytes and car-

[3] K. Sakai, unpublished data.

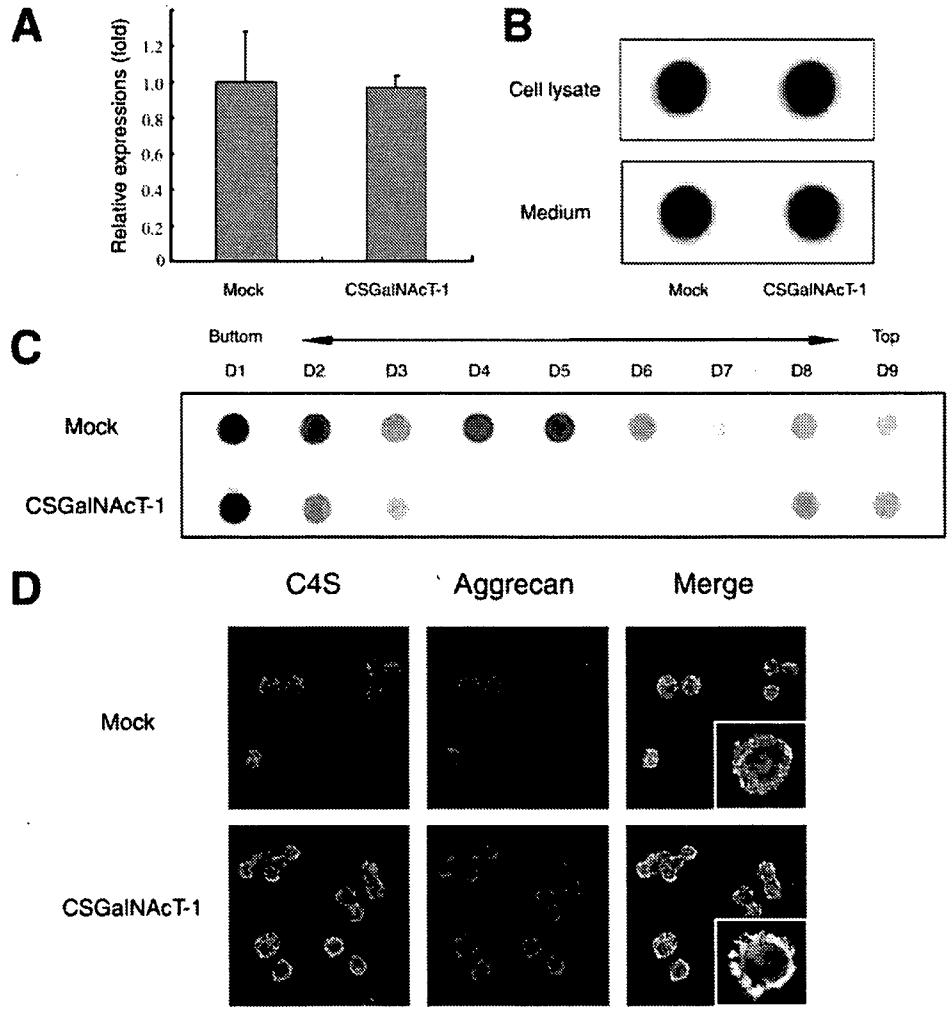

FIGURE 6. **Characterization of aggrecan in CSGalNAcT-1-overexpressing cells.** The aggrecan in CSGalNAcT-1-overexpressing cells contains a large amount of CS. *A*, mRNA levels of aggrecan core protein measured by real time RT-PCR. *B*, immunoblot of aggrecan core protein in cell lysates and conditioned medium. *C*, immunoblot analysis of aggrecan core protein after CsCl density gradient ultracentrifugation. Note that aggrecan in CSGalNAcT-1-overexpressing cells is mainly present in the bottom fractions (fractions 1 and 2), whereas that in mock-transfected cells is widely distributed in fractions 1–6. The density (g/ml) of each fraction is 1.638 for D1, 1.615 for D2, 1.600 for D3, 1.573 for D4, 1.525 for D5, 1.512 for D6, 1.465 for D7, 1.460 for D8, and 1.420 for D9, respectively. *D*, immunostaining for aggrecan core protein and chondroitin 4-sulfate (*C4S*). Chondroitin 4-sulfate stains stronger in the pericellular zone of CSGalNAcT-1-overexpressing cells than in the mock-transfected cells, whereas the aggrecan core protein stained at similar levels.

tilage. CSGalNAcT-1 expression correlated well with that of aggrecan core protein that provides acceptor sites for the glycosaminoglycan chains. CSGalNAcT-1 expression was closely associated with chondrocyte differentiation. Since CSGalNAcT-1 expression was diminished accordingly in the heterozygote and homozygote cmd cartilage, the expression of aggrecan core protein may regulate that of CSGalNAcT-1. Aggrecan core protein as substrate may be required for enzyme complex, and its decrease may deliver a feedback signal toward down-regulation of CSGalNAcT-1 expression. Alternatively, aggrecan in the cartilage matrix may maintain the chondrocyte phenotype, including high level expression of CSGalNAcT-1. Thus far, we have not identified *cis*-elements that are specific to chondrocyte differentiation in the promoter region of the CSGalNAcT-1 gene. The transcriptional regulation of this gene remains to be studied.

We demonstrated the presence of aggrecan with a larger number of attached CS chains in CSGalNAcT-1-overexpressing cells (Fig. 9). We designate this molecule "superaggrecan," since it would more efficiently contribute to cartilage function. Since CSGalNAcT-1 has stronger initiating activity than elongating activity (18), chain initiation may be the rate-limiting step in CS biosynthesis, and chondrocytes may have sufficient machinery for CS chain elongation following initiation. Indeed, overexpression of CSS-1, CSS-2, and CSGlcAT did not increase CS biosynthesis. The other enzyme involved in chain initiation, CSGalNAcT-2, showed consistent low expression in cartilage and has lower initiation activity than CSGalNAcT-1 (20), excluding any major involvement in cartilage CS biosynthesis. Enhanced CS biosynthesis by CSGalNAcT-1 overexpression suggests the presence of a large number of linkage regions as acceptor substrates in the native aggrecan. Although the aggrecan core protein has more than 100 putative Ser-Gly sequences of the CS attachment sites (2), approximately half of them may be attached only with the linkage tetrasaccharides. However, stubs of the linkage region have not been identified in aggrecan, although such stubs are present in a part-time CS proteoglycan thrombomodulin, an integral membrane glycoprotein expressed on endothelial cell surfaces (37). Recently, GlcAT-I, which transfers a GlcUA residue to the second Gal residue in the linkage region, has been shown to increase CS biosynthesis to ~1.5-fold (38). Thus, an immature linkage region may be present, and the enzyme complex that includes GlcAT-I and CSGalNAcT-1 may catalyze the completion of the linkage region and CS chain initiation.

Lines of evidence that support CSGalNAcT-1 as the critical enzyme for CS biosynthesis in various tissues as well as cartilage have been presented. Syndecan-4 in CSGalNAcT-1-overexpressing COS7 cells contains a large amount of CS (20). CSGalNAcT-1 overexpression in Balb/3T3 cells, a cell line established from normal mouse fibroblast cells, achieves ~5-fold CS synthesis.[3] Taken together, these observations strongly suggest that chain initiation by CSGalNAcT-1 is a critical step in the regulation of CS biosynthesis, and overexpression of the enzyme would substantially increase CS synthesis in various tissues.

To date, many approaches to promote cartilage regeneration have been attempted, including the treatment of mes-

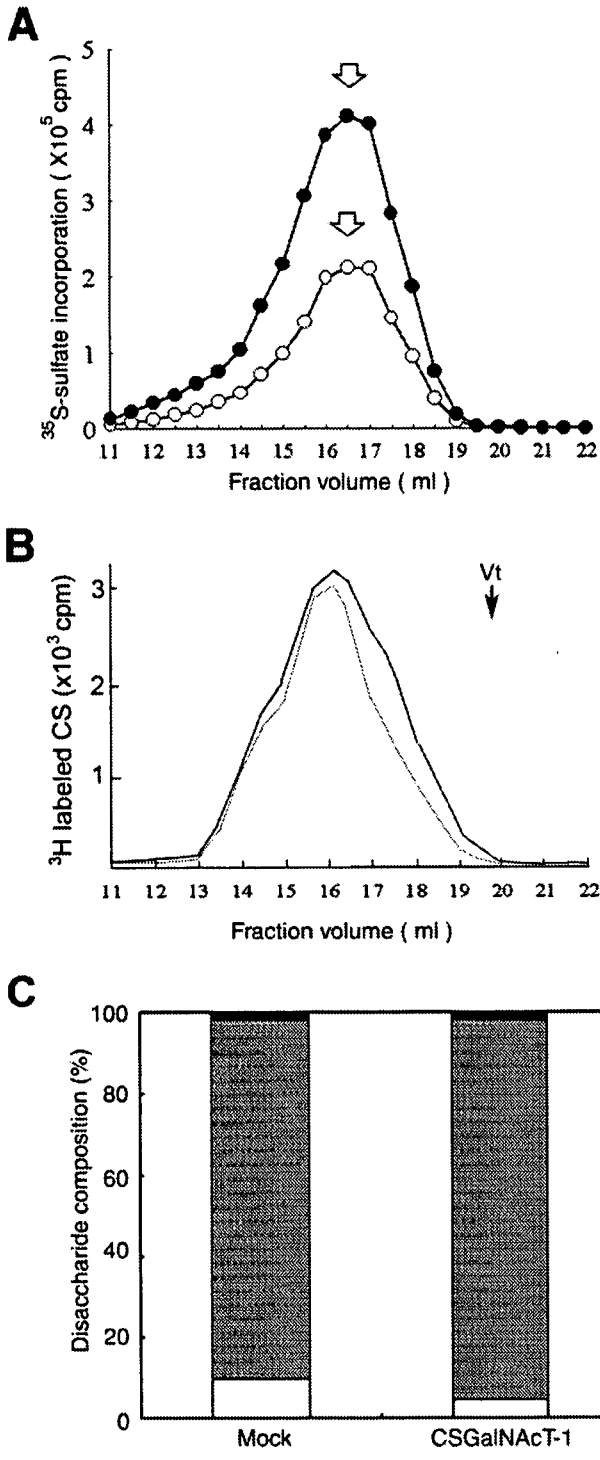

FIGURE 7. **Analysis of CS chains in CSGalNAcT-1-overexpressing cells.** *A*, elution profiles of Superose 6 gel chromatography. The cells were metabolically labeled with [^{35}S]sulfate for 24 h. Glycosaminoglycans, extracted as indicated under "Experimental Procedures," were applied to the Superose 6 column. The samples from CSGalNAcT-1-overexpressing cells (*closed circle*) and the mock transfectant cells (*open circle*) are shown. Note that two peaks are located at the same position (*arrows*). *B*, elution profiles of Superose 6 gel chromatography. CS-rich fractions prepared from the conditioned medium were labeled with ^{3}H-labeled sodium borohydride and were applied to Superose 6 column. The samples from CSGalNAcT-1-overexpressing cells (*thick line*) and the mock-transfectant cells (*narrow line*) are shown. Note that two peaks are at the same position. *Vt*, position of the total volume. *C*, disaccharide composition of CS in CSGalNAcT-1 and mock transfectants. HexA-GalNAc (*open bar*), HexA-GalNAc(4S) (*gray bar*), and others (*black bar*) are shown as a percentage of the saccharide content. HexA-GalNAc, HexA-GalNAc(4S), and the other disaccharides were observed to have similar ratios in both GSGalNAcT-1- and mock-transfected cells.

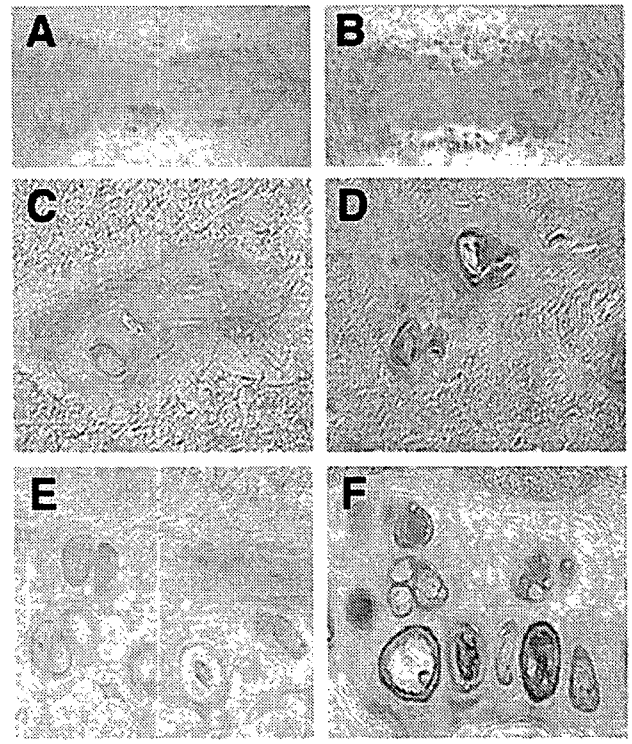

FIGURE 8. **Increased CS biosynthesis by *in vivo* gene delivery of CSGalNAcT-1.** Shown are histological sections of mouse intervertebral discs at 4 months of age, which were stained with Alcian blue (pH 1.0), 7 days after an injection of adenoviral particles. Low magnification of the intervertebral disc (*A* and *B*), higher magnification of nucleus pulposus (*C* and *D*), and the endplate (*E* and *F*) injected with mock (*A*, *C*, and *E*) and CSGalNAcT-1 (*B*, *D*, and *F*) adenovirus are shown. Note the intense Alcian blue staining in the pericellular zone of the nucleus pulposus cells in the disc and chondrocytes in the vertebral endplate of mice with CSGalNAcT-1 gene delivery compared with mice injected with the control adenovirus.

enchymal stem cells with growth factors to promote their differentiation into chondrocytes and the implantation of chondrocytes incorporated into scaffolds that maintain cellular phenotype and support the tissue structure (39–42). These interventions are based on the notion that aggrecan is synthesized only by chondrocytes and that it is essential for cartilage function. However, because of the difficulty in maintaining aggrecan synthesis in chondrocytes, regeneration of functional cartilage has not yet been achieved. In contrast to the above approaches, our research focused on CS as the critical factor that determines cartilage function and successfully generated superaggrecan. Since the turnover of aggrecan in cartilage is slow, with a half-life of approximately 10 years (43–45), the function of superaggrecan will most probably be maintained.

Adenoviral gene delivery of CSGalNAcT-1 enhanced *in vivo* CS synthesis in nucleus pulposus cells and endplate chondrocytes. In contrast, we have been unsuccessful in gene delivery to the articular cartilage (data not shown), although a recent similar study demonstrated increased CS expression in an articular cartilage explant (38). Since CS biosynthesis occurs in the Golgi apparatus (22), the addition of the enzyme to the tissue is ineffective, and overexpression in the cell is essential for this enzyme-based increase in CS levels. Effective gene delivery of CSGalNAcT-1 would be necessary to evaluate the prevention of cartilage destruction.

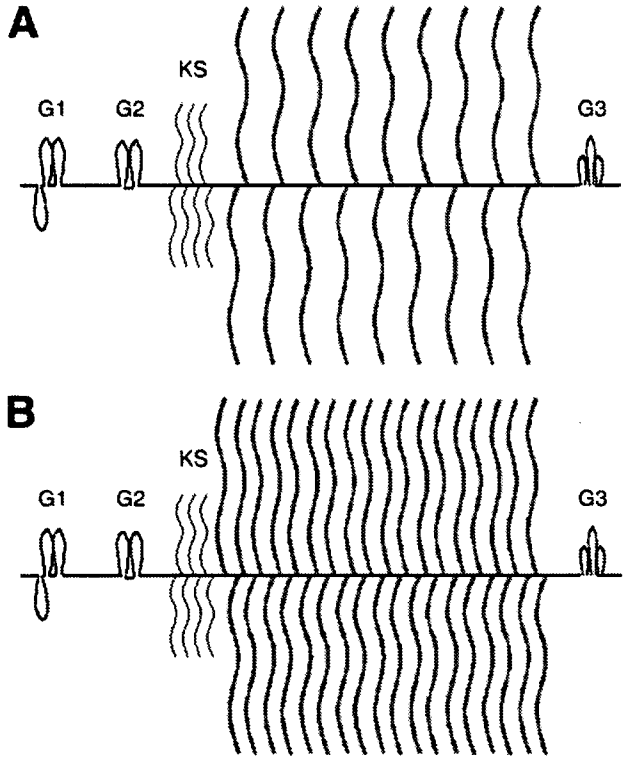

FIGURE 9. **A schematic diagram of aggrecan synthesized by control and CSGalNAcT-1-overexpressing chondrocytes.** *A*, native aggrecan; *B*, aggrecan in CSGalNAcT-1-overexpressing cells, which contains ~2.2-fold the number of CS chains attached to the core protein; designated "superaggrecan" (*blue*, CS chain). *G1*, G1 globular domain; *G2*, G2 globular domain; *G3*, G3 globular domain; *KS*, keratan sulfate.

In conclusion, this study identified the glycosyltransferase critical for CS biosynthesis and proposes a novel strategy for the treatment of cartilage degenerative disorders, distinct from cell-based approaches that focus on chondrocyte differentiation and aggrecan core protein expression. The effects of superaggrecan on chondrocyte homeostasis and its susceptibility to aggrecan-degrading proteinases remain to be performed.

Acknowledgments—We thank Dr. Rafrenie (Northern Ontario School of Medicine, Sudbury, Canada) for proofreading the manuscript, Drs. N. Sugiura and H. Habuchi for technical comments, Dr. H. Kitagawa for valuable discussion, and S. Hara for technical assistance.

REFERENCES

1. Watanabe, H., Yamada, Y., and Kimata, K. (1998) *J. Biochem. (Tokyo)* **124,** 687–693
2. Watanabe, H., Gao, L., Sugiyama, S., Doege, K., Kimata, K., and Yamada, Y. (1995) *Biochem. J.* **308,** 433–440
3. Doege, K. J., Garrison, K., Coulter, S. N., and Yamada, Y. (1994) *J. Biol. Chem.* **269,** 29232–29240
4. Plaas, A. H., Wong-Palms, S., Roughley, P. J., Midura, R. J., and Hascall, V. C. (1997) *J. Biol. Chem.* **272,** 20603–20610
5. Roughley, P., Martens, D., Rantakokko, J., Alini, M., Mwale, F., and Antoniou, J. (2006) *Eur. Cell. Mater.* **11,** 1–7
6. Bayliss, M. T. (1990) *Biochem. Soc. Trans.* **18,** 799–802
7. Dieppe, P. A., and Lohmander, L. S. (2005) *Lancet* **365,** 965–973
8. Creamer, P., and Hochberg, M. C. (1997) *Lancet* **350,** 503–508
9. Luoma, K., Riihimaki, H., Luukkonen, R., Raininko, R., Viikari-Juntura, E., and Lamminen, A. (2000) *Spine* **25,** 487–492
10. Andersson, G. B. (1999) *Lancet* **354,** 581–585
11. Silbert, J. E., and Sugumaran, G. (2002) *IUBMB Life* **54,** 177–186
12. Rohrmann, K., Niemann, R., and Buddecke, E. (1985) *Eur. J. Biochem.* **148,** 463–469
13. Kitagawa, H., Uyama, T., and Sugahara, K. (2001) *J. Biol. Chem.* **276,** 38721–38726
14. Kitagawa, H., Izumikawa, T., Uyama, T., and Sugahara, K. (2003) *J. Biol. Chem.* **278,** 23666–23671
15. Yada, T., Gotoh, M., Sato, T., Shionyu, M., Go, M., Kaseyama, H., Iwasaki, H., Kikuchi, N., Kwon, Y. D., Togayachi, A., Kudo, T., Watanabe, H., Narimatsu, H., and Kimata, K. (2003) *J. Biol. Chem.* **278,** 30235–30247
16. Yada, T., Sato, T., Kaseyama, H., Gotoh, M., Iwasaki, H., Kikuchi, N., Kwon, Y. D., Togayachi, A., Kudo, T., Watanabe, H., Narimatsu, H., and Kimata, K. (2003) *J. Biol. Chem.* **278,** 39711–39725
17. Gotoh, M., Yada, T., Sato, T., Akashima, T., Iwasaki, H., Mochizuki, H., Inaba, N., Togayachi, A., Kudo, T., Watanabe, H., Kimata, K., and Narimatsu, H. (2002) *J. Biol. Chem.* **277,** 38179–38188
18. Gotoh, M., Sato, T., Akashima, T., Iwasaki, H., Kameyama, A., Mochizuki, H., Yada, T., Inaba, N., Zhang, Y., Kikuchi, N., Kwon, Y. D., Togayachi, A., Kudo, T., Nishihara, S., Watanabe, H., Kimata, K., and Narimatsu, H. (2002) *J. Biol. Chem.* **277,** 38189–38196
19. Uyama, T., Kitagawa, H., Tamura Ji, J., and Sugahara, K. (2002) *J. Biol. Chem.* **277,** 8841–8846
20. Sato, T., Gotoh, M., Kiyohara, K., Akashima, T., Iwasaki, H., Kameyama, A., Mochizuki, H., Yada, T., Inaba, N., Togayachi, A., Kudo, T., Asada, M., Watanabe, H., Imamura, T., Kimata, K., and Narimatsu, H. (2003) *J. Biol. Chem.* **278,** 3063–3071
21. Uyama, T., Kitagawa, H., Tanaka, J., Tamura, J., Ogawa, T., and Sugahara, K. (2003) *J. Biol. Chem.* **278,** 3072–3078
22. Silbert, J. E., and Freilich, L. S. (1980) *Biochem. J.* **190,** 307–313
23. Watanabe, H., and Yamada, Y. (1999) *Nat. Genet.* **21,** 225–229
24. Atsumi, T., Miwa, Y., Kimata, K., and Ikawa, Y. (1990) *Cell Differ. Dev.* **30,** 109–116
25. Kamiya, N., Jikko, A., Kimata, K., Damsky, C., Shimizu, K., and Watanabe, H. (2002) *J. Bone. Miner. Res.* **17,** 1832–1842
26. Matsumoto, K., Kamiya, N., Suwan, K., Atsumi, K., Shimizu, K., Shinomura, T., Yamada, Y., Kimata, K., and Watanabe, H. (2006) *J. Biol. Chem.* **281,** 18257–18263
27. Nogami, H., Suzuku, H., Habuchi, H., Ishiguro, N., Iwata, H., and Kimata, K. (2004) *J. Biol. Chem.* **279,** 8219–8229
28. Toyoda, H., Kinoshita-Toyoda, A., and Selleck, S. B. (2000) *J. Biol. Chem.* **275,** 2269–2275
29. DeLise, A. M., Fischer, L., and Tuan, R. S. (2000) *Osteoarthritis Cartilage* **8,** 309–334
30. Shibata, S., Fukada, K., Imai, H., Abe, T., and Yamashita, Y. (2003) *J. Anat.* **203,** 425–432
31. Shukunami, C., Shigeno, C., Atsumi, T., Ishizeki, K., Suzuki, F., and Hiraki, Y. (1996) *J. Cell Biol.* **133,** 457–468
32. Watanabe, H., Kimata, K., Line, S., Strong, D., Gao, L. Y., Kozak, C. A., and Yamada, Y. (1994) *Nat. Genet.* **7,** 154–157
33. Watanabe, H., Nakata, K., Kimata, K., Nakanishi, I., and Yamada, Y. (1997) *Proc. Natl. Acad. Sci. U. S. A.* **94,** 6943–6947
34. Choi, H. U., Meyer, K., and Swarm, R. (1971) *Proc. Natl. Acad. Sci. U. S. A.* **68,** 877–879
35. Oegema, T. R., Jr., Hascall, V. C., and Dziewiatkowski, D. D. (1975) *J. Biol. Chem.* **250,** 6151–6159
36. Silbert, J. E. (1996) *Glycoconj. J.* **13,** 907–912
37. Nadanaka, S., Kitagawa, H., and Sugahara, K. (1998) *J. Biol. Chem.* **273,** 33728–33734
38. Venkatesan, N., Barre, L., Benani, A., Netter, P., Magdalou, J., Fournel-Gigleux, S., and Ouzzine, M. (2004) *Proc. Natl. Acad. Sci. U. S. A.* **101,** 18087–18092
39. Martinek, V., Ueblacker, P., and Imhoff, A. B. (2003) *J. Bone Joint. Surg. Br.* **85,** 782–788
40. Kuo, C. K., Li, W. J., Mauck, R. L., and Tuan, R. S. (2006) *Curr. Opin. Rheumatol.* **18,** 64–73

41. Masuda, K., Oegema, T. R., Jr., and An, H. S. (2004) *Spine* **29,** 2757–2769
42. Anderson, D. G., Albert, T. J., Fraser, J. K., Risbud, M., Wuisman, P., Meisel, H. J., Tannoury, C., Shapiro, I., and Vaccaro, A. R. (2005) *Spine* **30,** S14–S19
43. Maroudas, A., Bayliss, M. T., Uchitel-Kaushansky, N., Schneiderman, R., and Gilav, E. (1998) *Arch. Biochem. Biophys.* **350,** 61–71
44. Sivan, S. S., Tsitron, E., Wachtel, E., Roughley, P. J., Sakkee, N., van der Ham, F., Degroot, J., Roberts, S., and Maroudas, A. (2006) *J. Biol. Chem.* **281,** 13009–13014
45. Maroudas, A. (1975) *Philos. Trans. R. Soc. Lond. B Biol. Sci.* **271,** 293–313

THE JOURNAL OF BIOLOGICAL CHEMISTRY VOL. 282, NO. 27, pp. 19589–19597, July 6, 2007

Essential Role of Heparan Sulfate 2-*O*-Sulfotransferase in Chick Limb Bud Patterning and Development*[S]

Received for publication, November 20, 2006, and in revised form, May 4, 2007 Published, JBC Papers in Press, May 10, 2007, DOI 10.1074/jbc.M610707200

Takashi Kobayashi[‡], Hiroko Habuchi[‡], Koji Tamura[§], Hiroyuki Ide[§], and Koji Kimata[‡1]

From the [‡]Institute for Molecular Science of Medicine, Aichi Medical University, Nagakute, Aichi 480-1195, Japan and [§]Department of Developmental Biology and Neurosciences, Graduate School of Life Sciences, Tohoku University, Aobayama Aobaku, Sendai 980-8578, Japan

The interactions of heparan sulfate (HS) with heparin-binding growth factors, such as fibroblast growth factors (FGFs), depend greatly on the chain structures. *O*-Sulfations at various positions on the chain are major factors determining HS structure; therefore, *O*-sulfation patterns may play a crucial role in controlling the developmental and morphogenetic processes of various tissues and organs by spatiotemporally regulating the activities of heparin-binding growth factors. In a previous study, we found that HS-2-*O*-sulfotransferase is strongly expressed throughout the mesoderm of chick limb buds during the early stages of development. Here we show that inhibition of HS-2-*O*-sulfotransferase in the prospective limb region by small inhibitory RNA resulted in the truncation of limb buds and reduced *Fgf-8* expression in the apical ectodermal ridge. The treatment also reduced *Fgf-10* expression in the mesenchyme. Moreover 2-*O*-sulfated HS, normally abundant in the basement membranes and mesoderm under ectoderm in limb buds, was significantly reduced in the treated buds. Phosphorylation levels of ERK and Akt were up-regulated in such truncated buds. Thus, we have shown for the first time that 2-*O*-sulfation of HS is essential for the FGF signaling required for limb bud development and outgrowth.

Chick limb bud is a useful model of limb pattern formation, which involves various growth factors and morphogens such as fibroblast growth factor (FGF),[2] hedgehog, wingless/Wnt, and bone morphogenetic proteins (1–4). Limb bud initiation requires reciprocal interactions between a specialized ectodermal structure called the apical ectodermal ridge (AER) and the underlying mesoderm (5, 6). At the time of limb initiation, in stages 13–15 of the chick embryo, *Fgf-8* in the intermediate mesoderm induces *Fgf-10* expression in the lateral plate mesoderm (LPM) of the prospective limb region. FGF-10 produced in the prospective limb mesoderm then induces *Fgf-8* expression in the overlying surface ectoderm (AER). FGF-8 secreted from AER maintains *Fgf-10* expression in the underlying mesoderm. This FGF signaling loop establishes the maintenance of AER and outgrowth of limb buds. FGF-8 also contributes to *Shh* induction, which in turn induces *Fgf-4* expression in the AER and maintains AER function in the posterior underlying mesoderm called the zone of polarizing activity (7, 8).

Although growth factors and morphogens are required for limb bud development and patterning, it is unclear how their signaling and distribution are regulated. Heparan sulfate proteoglycans, which are ubiquitous on the cell surface and in the extracellular matrix including basement membranes, are important regulators of such growth factor signaling and distribution (9–11). For example, chicken syndecan-3 is expressed throughout the distal mesenchymal cells and plays a role in limb bud outgrowth by controlling FGF signaling between the AER and mesoderm (12). Heparan sulfate proteoglycans play such roles by interacting with these growth factors (13–15); however, it is unclear what role HS chains play in these processes, although HS chains are known to interact with a variety of heparin-binding growth factors (HBGFs) such as FGF.

In FGF signaling, the ternary complex composed of HS chains, FGF family molecules, and FGF receptors (FGFRs) is formed on the cell surface (16–18). Specificities of interactions between heparan sulfate proteoglycan and ligand molecules are thought to reside in the fine structures of HS chains with specific sequences consisting of highly sulfated monosaccharides (*N*-, 2-*O*-, and/or 6-*O*-sulfated) (9, 19, 20). In fact, the different *O*-sulfation patterns of HS chains are involved in interactions with FGF family molecules (21–23). These fine structures are generated by the following modification reactions with specific enzymes after the backbone chain of HS is synthesized by the addition of alternating D-glucuronic acid and *N*-acetyl-D-glucosamine (GlcNAc) residues from the respective UDP sugars by EXT family proteins (24): GlcNAc *N*-deacetylation and *N*-sulfation by *N*-deacetylase/*N*-sulfotransferase, C-5 epimerization of D-glucuronic acid residues to iduronic acid by C-5 epimerase, and *O*-sulfations at various places that take place first at C-2 of IdoA and D-glucuronic acid by heparan sulfate 2-*O*-sulfotransferase (HS2ST), subsequently at C-6 of GlcNAc and *N*-sulfate-

* This work was supported by Grant-in-aid for Scientific Research on Priority Areas 14082206 from the Ministry of Education, Culture, Sports, Science and Technology of Japan and by a special research fund from the Seikagaku Corp. The costs of publication of this article were defrayed in part by the payment of page charges. This article must therefore be hereby marked "*advertisement*" in accordance with 18 U.S.C. Section 1734 solely to indicate this fact.

[S] The on-line version of this article (available at http://www.jbc.org) contains supplemental Fig. 1.

[1] To whom correspondence should be addressed. Tel.: 81-561-62-3311 (ext. 2088); Fax: 81-561-63-3532; E-mail: kimata@amugw.aichi-med-u.ac.jp.

[2] The abbreviations used are: FGF, fibroblast growth factor; HS, heparan sulfate; HS2ST, heparan sulfate 2-*O*-sulfotransferase; HS6ST, heparan sulfate 6-*O*-sulfotransferase; HBGF, heparin-binding growth factor; FGFR, fibroblast growth factor receptor; AER, apical ectodermal ridge; LPM, lateral plate mesoderm; RNAi, RNA interference; siRNA, small inhibitory RNA; esiRNA, endonuclease-digested small inhibitory RNA; ERK, extracellular signal-regulated kinase; pERK, phosphorylated ERK; pAkt, phosphorylated Akt; PBS, phosphate-buffered saline; GFP, green fluorescent protein; MAPK, mitogen-activated protein kinase; EXT, extosis.

D-glucosamine units by heparan sulfate 6-*O*-sulfotransferases (HS6STs), and lastly at C-3 of *N*-sulfate-D-glucosamine residues by heparan sulfate 3-*O*-sulfotransferases (25–27).

O-Sulfation residues and patterns have been shown to be critical to HS function in several developmental processes. For example, gene trap mutation of HS2ST in mice causes renal agenesis, eye and skeleton defects, and neonatal lethality (28). HS6ST-1 null mice die between embryonic day 15.5 and the perinatal stage and show a reduction in the number of fetal microvessels in the labyrinthine zone of the placenta (29). In addition, a recent report on mutant HS2ST and HS6ST-1 mice showed defects of specific axon guidance at the optic chiasm (30). Morpholino-mediated knockdown of HS6ST in zebrafish results in disruption of somitic muscle development and defects in the branching morphogenesis of the caudal vein (31, 32). Inhibition of *Drosophila* HS6ST expression by RNA interference (RNAi) reduces FGF signaling activity and disrupts the primary branching of the tracheal system (33).

Previously we showed distinctive expression patterns of HS *O*-sulfotransferases in developing chick limb buds (34). HS6ST-1 and HS6ST-2 transcripts are preferentially localized in the anterior and posterior proximal regions of the limb bud, respectively, whereas HS2ST transcripts are distributed rather uniformly throughout the bud. HS sulfation patterns in chick limb buds correspond exactly with these expression patterns (34). Thus, specific HS sulfation patterns may regulate the development and patterning of limb buds by binding to growth factors and morphogens. In this study, we examined the role of 2-*O*-sulfation in the morphogenesis of the chicken limb. Electroporation of RNA duplexes (RNAi technique) is effective at suppressing the expression of target genes in chick embryos (35). Disruption of the HS2ST gene by small inhibitory RNA (siRNA) reduced 2-*O*-sulfation levels and led to the abnormal development of limb buds, which showed less expression of both *Fgf-8* and *Fgf-10* accompanied by the up-regulation of phosphorylation of both ERK and Akt. Taken together, these results suggest that reducing 2-*O*-sulfate residues affect limb bud formation and outgrowth.

EXPERIMENTAL PROCEDURES

Preparation of Chicken Embryos—Fertile White Leghorn chicken eggs were obtained from Takeuchi Farm (Nara, Japan), incubated in humidified air at 38 °C, and staged according to Hamburger and Hamilton (36).

RNAi—Double-stranded RNA corresponding to the HS2ST open reading frame sequence was prepared and then digested with RNase III. Chicken HS2ST open reading frame was subcloned into pBluescriptII KS(−) (Stratagene, La Jolla, CA) before transcribing sense and antisense single-stranded RNA from T3 and T7 RNA polymerase promoters. RNA was incubated with DNase I to degrade the template DNA. Sense and antisense RNA were annealed into duplexes by combining equal amounts of each type of RNA, then denatured at 95 °C for 5 min, and incubated at 37 °C overnight. Annealed duplexes were incubated with RNase I (Ambion, Austin, TX) at 37 °C for 30 min and then treated with phenol-chloroform. The purified duplexes were resuspended in distilled water. To generate endonuclease-digested small inhibitory RNA (esiRNA), double-stranded RNA was incubated with RNase III (New England Biolabs, Beverly, MA) at 37 °C for 30 min. The reaction products were purified with siRNA Purification Units (Ambion), then precipitated with ethanol, and resuspended in distilled water. As controls for the siRNA treatment, siRNA mixtures for luciferase, the gene of which is derived from pGL3-Basic (Promega, Madison, WI), were prepared by the same procedure.

In Ovo Electroporation—For electroporation experiments, eggs were opened after 2 days of incubation at 38 °C, corresponding to stage 13-14, and a solution of India ink diluted in Tyrode's solution was applied below the blastoderm to enhance contrast. The vitellin membrane overlying the presumptive forelimb region was also carefully removed using a fine tungsten needle. RNA solutions containing 0–700 ng/μl esiRNA, 0.1% fast green, and 2 μg/μl pEGFP-N1 (Clontech) were injected into the LPM of the presumptive right forelimb region of embryos, and several drops of Tyrode's solution were added after injection. Electrodes were placed above (cathode) and below (anode) the forelimb region containing the injected RNA, and electroporation (three 15-V, 25-ms pulses) was performed with ElectroSquarePorator T820 (BTX; Inovio Biomedical Corp., San Diego, CA). Experimental embryos were observed and/or harvested 16–48 h after electroporation. For cryosections, embryos were fixed in 4% paraformaldehyde, PBS at 4 °C overnight and then incubated in 30% sucrose, PBS at 4 °C for 2–12 h. Embryos were embedded in OCT compound (Sakura, Tokyo, Japan), and 10-mm-thick cryosections were made.

In Situ Hybridization—Whole-mount and section *in situ* hybridization was performed as described previously with slight modifications (34, 37–39). For whole-mount *in situ* hybridization, embryos were fixed in 4% paraformaldehyde, PBS overnight and then digested with 1 μg/ml proteinase K in PBS containing 0.1% Tween 20 at 20 °C for 15 min. Hybridization was performed at 65 °C in 5× SSC, 50% (v/v) formamide, 1% (w/v) SDS, 50 μg/ml heparin, and 50 μg/ml yeast tRNA using digoxigenin-labeled RNA as a probe.

In Situ FGF-2 Binding Assay and Immunohistochemistry—For *in situ* detection of 2-*O*-sulfated HS, we used an exogenous FGF-2 binding assay (40). Cryosections were air-dried and then washed with PBS. To remove endogenous HS-bound molecules, sections were incubated with 2 M NaCl, PBS at room temperature for 10 min and then washed three times with PBS. When necessary, sections were treated with a mixture of heparitinases (Seikagaku Corp., Tokyo, Japan) at 37 °C for 2 h. Sections were incubated with 5–30 nM recombinant human FGF-2 (Roche Applied Science) at 4 °C overnight followed by blocking for 1 h at room temperature with PBS containing 10% bovine serum albumin (Sigma). After five washes with PBS, FGF-2 binding was analyzed using an anti-FGF-2 monoclonal antibody (05-118; Upstate Biotechnology, Lake Placid, NY) and Alexa-conjugated secondary antibody (Molecular Probes, Eugene, OR). HS was detected with 3G10 antibody (Seikagaku Corp.) and secondary antibody.

Western Blot Analysis—For Western blot analysis, tissue lysates of stage 22-23 limb buds were subjected to 10% SDS-polyacrylamide gel electrophoresis and transferred to a polyvinylidene difluoride membrane. The blots were incubated with

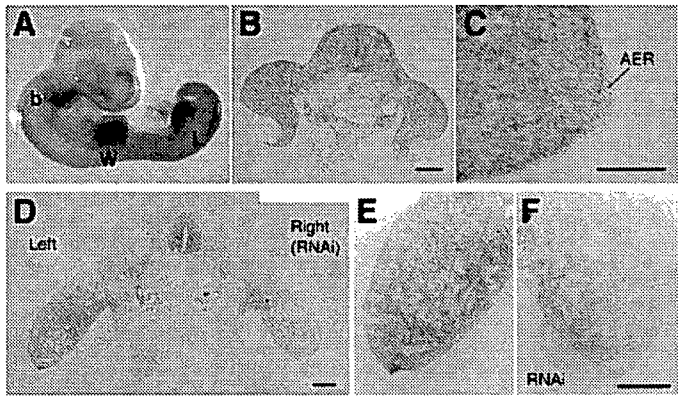

FIGURE 1. **Expression pattern of chicken HS2ST mRNA.** *A*, whole-mount *in situ* hybridization of stage 23 embryo. A high level of HS2ST transcripts was detected in wing (*W*) and leg (*L*) buds and in the branchial arches (*b*). *B* and *C*, *in situ* hybridization of transverse sections of stage 22 wing buds. HS2ST is expressed weakly in the AER and ectoderm (*C*). *D–F*, *in situ* hybridization of transverse sections of siRNA-injected embryos. HS2ST siRNA was injected into the prospective region of the right wing bud of stage 13 embryos (*D*). Treated embryos were fixed at stage 23-24 (45 h after treatment). The right bud (*F*) showed lower levels of HS2ST mRNA compared with the untreated left bud (*E*). *Scale bars* in *B*, *D*, and *F*, 200 μm; *scale bar* in *C*, 50 μm.

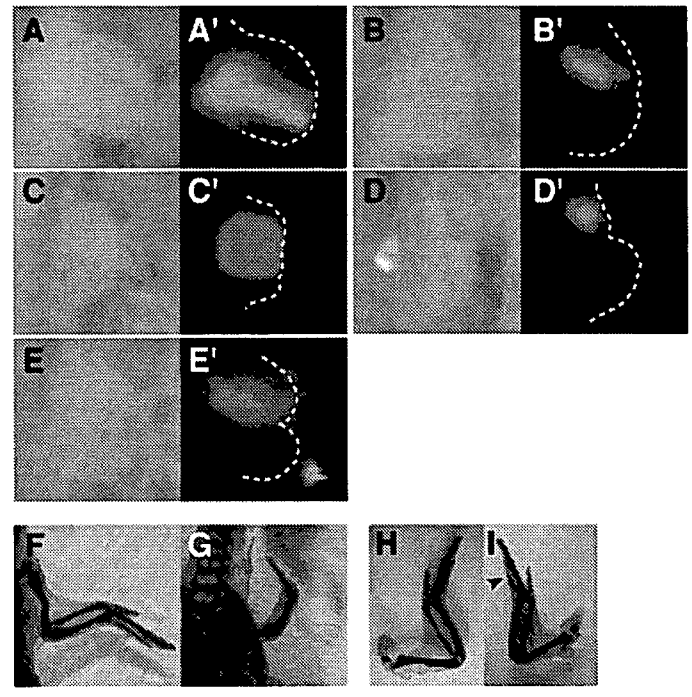

FIGURE 2. **Abnormal limb bud formation by HS2ST RNAi.** *A–E*, HS2ST esiRNA- or PBS-injected stage 22-23 limb bud. HS2ST siRNA mixtures (150 ng/μl) or PBS was injected, via electroporation, into the lateral plate mesoderm of the prospective right wing bud region of stage 13-14 embryos. *A'–E'*, GFP signals, derived from coelectroporated pEGFP-N1, indicated the siRNA-injected region. *A*, PBS-injected control samples had almost normal limb buds. *B–E*, HS2ST esiRNA-injected samples showed truncated limb buds. *B*, mildly truncated limb; *C*, moderately truncated limb; *D*, severely truncated limb; and *E*, indented limb. *F–I*, Alcian blue staining of skeletal patterns in HS2ST esiRNA-injected limbs revealed their abnormalities. *G*, severely affected right forelimb showing an abnormal skeletal pattern compared with untreated left forelimb (*F*). *I*, mildly affected right forelimb showing a defective digit (*arrowhead*) and size reduction compared with uninjected left forelimb (*H*).

10% skim milk in Tris-buffered saline/Tween 20 (TBST; Tris-buffered saline containing 0.1% Tween 20) and probed with anti-phosphorylated ERK (pERK) antibody (catalog number 9106; Cell Signaling Technology, Beverly, MA), anti-ERK antibody (catalog number 9102; Cell Signaling Technology), anti-phosphorylated Akt (pAkt) antibody (catalog number 9275; Cell Signaling Technology), or anti-actin antibody (catalog number A2066; Sigma) diluted with 1% skim milk in TBST. The signal was visualized using horseradish peroxidase-conjugated secondary antibody and enhanced chemiluminescence (Western Lighting Plus; PerkinElmer Life Sciences) according to the manufacturer's instructions.

Ligand and Carbohydrate Engagement Assays—In situ binding of the FGF·FGFR complex to heparan sulfate in the assay enables us to detect HS structure alterations (41, 42). The frozen sections were incubated in 2 M NaCl, PBS for 10 min followed by treatment with 10% BSA, PBS to block nonspecific binding. Slides were then incubated with 10–30 nM FGF-8 or FGF-10 (Peprotech Inc., Rocky Hill, NJ) together with 10–20 nM FGFR2b-Fc or FGFR2c-Fc (R&D Systems, Minneapolis, MN), respectively, which were fused with the human IgG Fc domain, at 4 °C overnight. After five washes with PBS, the bound FGFR-Fc was detected using a Cy3-conjugated anti-human Fc IgG secondary antibody (Chemicon International Inc., Temecula, CA).

RESULTS

Expression Patterns of HS2ST—HS2ST is highly expressed in the developing limb buds of chick embryos (34). Whole-mount *in situ* hybridization showed that HS2ST transcripts were localized uniformly throughout both wing and leg buds at stage 23 (Fig. 1*A*). In a transverse section of the wing bud region, HS2ST expression was strong in the mesenchyme and weak (but significant) in the overlying ectoderm including the AER (Fig. 1, *B* and *C*). This characteristic expression pattern suggests that HS2ST is deeply involved in limb bud development.

Abnormal Limb Bud Development and Outgrowth by HS2ST RNAi—To investigate the role of 2-*O*-sulfated HS in growth factor signaling in limb bud development, siRNA mixtures were transfected into the LPM of the prospective right forelimb region in stage 13-14 embryos via electroporation. HS2ST esiRNA-injected limbs caused abnormal development 2 days after the operation (Fig. 2, *B–E*), whereas PBS-injected limbs showed less abnormality (Fig. 2*A*). The abnormal limb buds were truncated and reduced in size (Fig. 2, *B–D*) or occasionally indented (Fig. 2*E*). When higher concentrations of esiRNA were injected, severe abnormal phenotypes were observed in the limb buds with higher frequency (Table 1). Green fluorescent protein (GFP) signals derived from coelectroporated pEGFP-N1 were observed around truncated regions of injected limb buds (Fig. 2, *B–E*). The skeletal pattern of mild affected limb at 9 days showed a defective digit and shorter structure compared with the uninjected control left limb (Fig. 2, *H* and *I*). Severely truncated buds showed little outgrowth and a markedly affected cartilage pattern at 9 days (Fig. 2, *D*, *F*, and *G*).

Luciferase esiRNA-injected buds showed a low frequency of abnormalities similar to that in the buffer-injected control (Table 1). For example, 150 ng/μl HS2ST esiRNA-injected buds had a higher frequency of abnormalities (26.5%) than 300 ng/μl luciferase esiRNA-injected buds (13.0%). Although it is known that RNAi techniques sometimes cause off-target effects, it is

TABLE 1
Frequency and severity of truncation of siRNA-injected limbs at stage 22-23

Injection		Severity of truncation[a]				
ng/ml	No.	Total	Mild	Moderate	Severe	Indentation
HS2ST esiRNA						
700	55	27 (49.1%)	12 (14.8%)	5 (18.5%)	4 (44.4%)	6 (22.2%)
450	37	12 (32.4%)	2 (33.3%)	4 (16.7%)	2 (16.7%)	4 (33.3%)
250	62	16 (25.8%)	7 (56.3%)	9 (43.7%)	0 (0%)	0 (0%)
150	78	20 (25.64%)	7 (50.0%)	10 (35.0%)	1 (5.0%)	2 (10.0%)
Luciferase esiRNA						
700	18	4 (22.2%)	3 (25.0%)	1 (75.0%)	0 (0%)	0 (0%)
300	23	3 (13.0%)	2 (33.3%)	1 (66.7%)	0 (0%)	0 (0%)
Buffer (PBS)						
0	84	11 (13.1%)	8 (27.3%)	3 (72.7%)	0 (0%)	0 (0%)

[a] Typical examples are shown in Fig. 2, *B–F*.

unlikely that the truncation is due to such effects. Furthermore the frequency of severe phenotypes in these controls was significantly less than that in HS2ST esiRNA-injected buds (Table 1). These results suggest that the injection of HS2ST esiRNA specifically caused truncation of the limb buds. In addition, HS2ST transcripts were reduced in HS2ST RNAi limb buds compared with untreated buds (Fig. 1, *D–F*). No reduction of HS2ST mRNA was observed in control limb buds (data not shown). These results indicate that siRNA mixtures effectively reduce HS2ST transcripts.

Alteration of HS Structures by HS2ST RNAi—We then examined whether the abnormal morphology of limb buds resulted from the loss of 2-*O*-sulfate residues in HS. Because no suitable antibodies for the detection of 2-*O*-sulfate residues in HS are available, we took advantage of the following binding properties of exogenous FGF-2 to HS to determine the distribution of 2-*O*-sulfated HS in tissues (40). We have shown that 2-*O*-sulfated HS is sufficient to bind FGF-2 (21). We pretreated the limb bud sections with 2 M NaCl to remove endogenous HBGFs, including FGF-2, bound to HS and then stained the sections with exogenous FGF-2 in combination with anti-FGF-2 antibody (Fig. 3 and supplemental Fig. 1). In the normal limb bud at stage 23, exogenous FGF-2 was strongly bound to the basement membranes and mesenchyme underneath the ectoderm (Fig. 3*B* and supplemental Fig. 1). These staining patterns coincided with HS distribution in the limb detected by 3G10 antibody (Fig. 3*A* and supplemental Fig. 1). When sections were treated with heparitinases before applying FGF-2, the FGF-2 binding region was markedly reduced, suggesting that exogenous FGF-2 binds specifically to HS (supplemental Fig. 1). These results indicate that 2-*O*-sulfated HS is abundant in the basement membranes and mesenchyme under the ectoderm in the developing limb bud. We then tested FGF-2 binding activity in siRNA-injected limb buds at stage 23 (Fig. 3). In RNAi-treated limb buds, exogenous FGF-2 bound only weakly to the truncated region compared with the unaffected region, whereas HS distributions themselves were not affected (Fig. 3, *E–H*). We could not see such a decrease of exogenous FGF-2 binding in luciferase RNAi-treated limb buds (data not shown). These results show that HS2ST RNAi also reduced 2-*O*-sulfation and FGF-2 binding. Interestingly 2-*O*-sulfation was significantly reduced in the basement membranes (Fig. 3, *E* and *F*, *arrowheads*). The decrease of 2-*O*-sulfation in the basement membranes could affect the movement of HBGFs between the mesoderm and ectoderm.

Effects on FGF Signaling Loop—To investigate whether HS2ST RNAi disrupted FGF signaling during limb bud development, we examined *Fgf-8* expression using whole-mount *in situ* hybridization of stage 22-23 limb buds (Fig. 4). A marked reduction of *Fgf-8* transcripts was observed in truncated buds by siRNA injection, whereas *Fgf-8* is expressed in the AER of untreated buds (Fig. 4, *A* and *B*). *Shh*, which is induced by FGF-8 signaling, was also reduced in limbs that showed decreased *Fgf-8* expression (Fig. 4*B*, *arrowhead*). In some cases (4 of 13 samples), the reduction of *Fgf-8* expression was also observed even in HS2ST esiRNA-injected but almost normally developed limb buds (Fig. 4*C*); however, no such reduction was observed in luciferase esiRNA-injected limb buds (11 samples).

We also examined Fgf expression in early developmental stages. Chick wing buds develop and grow at stages 18 and 19 at which point *Fgf-8* expression is detectable in the ectoderm (43). In the present study, *Fgf-8* expression was significantly reduced in the ectoderm of RNAi-treated limb buds compared with the untreated opposite limb bud (Fig. 5, *A* and *B*). In a few cases, *Fgf-8* expression was almost undetectable at this stage (Fig. 5*B*, *arrow*). As *Fgf-8* expression is induced by FGF-10 derived from the mesoderm and *Fgf-10* expression is maintained by FGF-8 derived from the AER (5, 6), we examined *Fgf-10* expression in RNAi-treated limb buds at similar stages. Similar to *Fgf-8*, *Fgf-10* expression in the mesoderm was also reduced in siRNA-injected buds (Fig. 5, *C* and *D*). Taken together, these results suggest that a reduction of 2-*O*-sulfated HS down-regulates both *Fgf-8* and *Fgf-10* expression in the developing limb bud.

Up-regulation of ERK and Akt Pathway—The intracellular response to FGFs is mediated by several signal transduction pathways including the MAPK/ERK and phosphatidylinositol 3-OH-kinase/Akt pathways. Recently both pathways have been shown to be essential for limb bud development and patterning (44–46). We examined the activation of ERK and Akt, which are activated in the MAPK and phosphatidylinositol 3-OH-kinase pathways, respectively. We dissected stage 23 esiRNA-injected right limb buds and untreated opposite left limb buds and probed for pERK, ERK, and pAkt by Western blot analysis. The truncated limb buds among those treated with HS2ST esiRNA showed approximately 2 times higher pERK levels than those of the untreated buds, although total ERK levels were not altered between the RNAi-treated and untreated buds (Fig. 6, *A* and *B*, *Group 1*). Similarly pAkt was also increased about 2-fold in the HS2ST RNAi limb buds (Fig. 6, *A* and *B*). No up-regulation of the phosphorylation of ERK and Akt was observed in

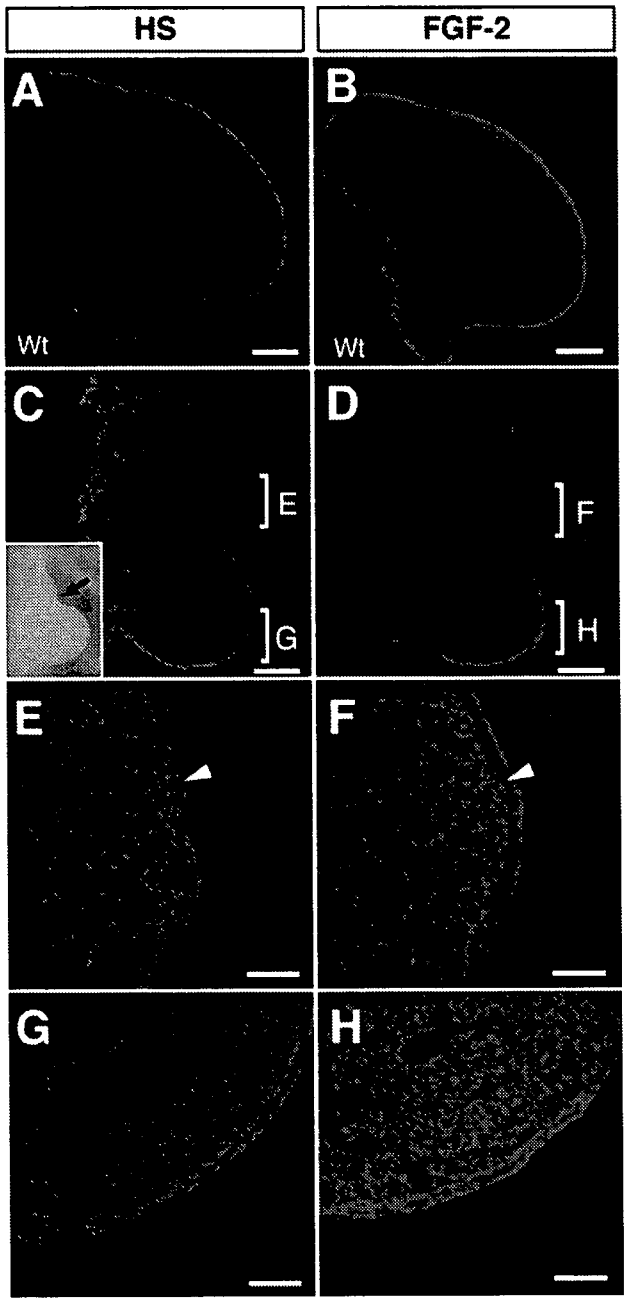

FIGURE 3. **Alteration of 2-*O*-sulfated HS by HS2ST RNAi.** *A* and *C*, HS was detected by 3G10 antibody. *B* and *D*, the 2-*O*-sulfated HS was detected as described under "Experimental Procedures." Longitudinal sections of limb buds (removal of endogenous HBGFs by treatment with 2 M NaCl) were exposed to exogenous FGF-2 and then probed with anti-FGF-2 antibody. The *top* of each figure shows the anterior region, and the *bottom* shows the posterior. *A* and *B*, normal limb buds at stage 23. *C* and *D*, HS2ST siRNA-injected limb bud (450 ng/μl) at stage 23 (45 h after treatment). The anterior half of the bud was truncated by RNAi treatment (*arrow* in *C*, *inset*). *E–H*, magnified images of *C* and *D*. FGF-2 binding activity was reduced in the siRNA-injected region (*F*) compared with unaffected regions (*H*), whereas HS distributions were not different between injected (*E*) and untreated regions (*G*). The basement membranes also showed a marked reduction in FGF-2 binding (compare *arrowheads* in *E* and *F*). *Scale bars* in *A–D*, 200 μm; *scale bars* in *E–H*, 20 μm. *Wt*, wild type.

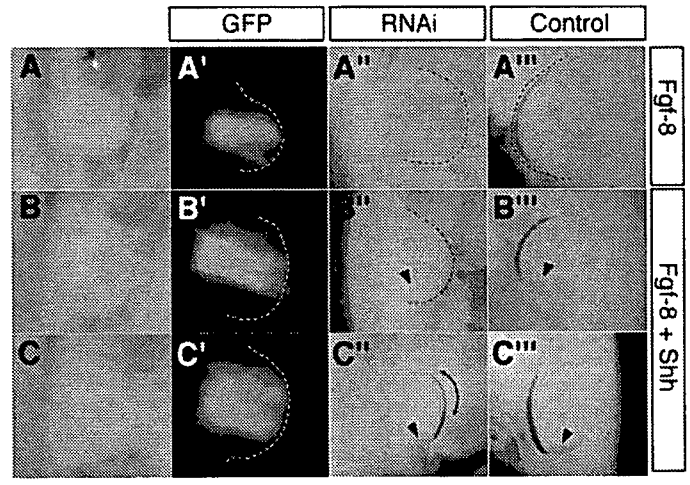

FIGURE 4. **Abnormal limb buds showed lower *Fgf-8* and *Shh* expression.** *A–C*, the expression patterns of *Fgf-8* and *Shh* in stage 23 embryos were detected by whole-mount *in situ* hybridization. *A'–C'*, GFP signals, which were derived from coelectroporated pEGFP-N1, indicated the siRNA-injected regions. *A''–C''*, right wing buds injected with 150 ng/μl esiRNA. *A'''–C'''*, the corresponding untreated left buds. *A*, moderately truncated and size-reduced limb bud. *B*, moderately truncated limb bud. *C*, almost normally developed limb bud. *Fgf-8* expression is partially reduced in the anterior region of AER (*arch*). *Arrowheads* in *B* and *C* indicate *Shh* expression.

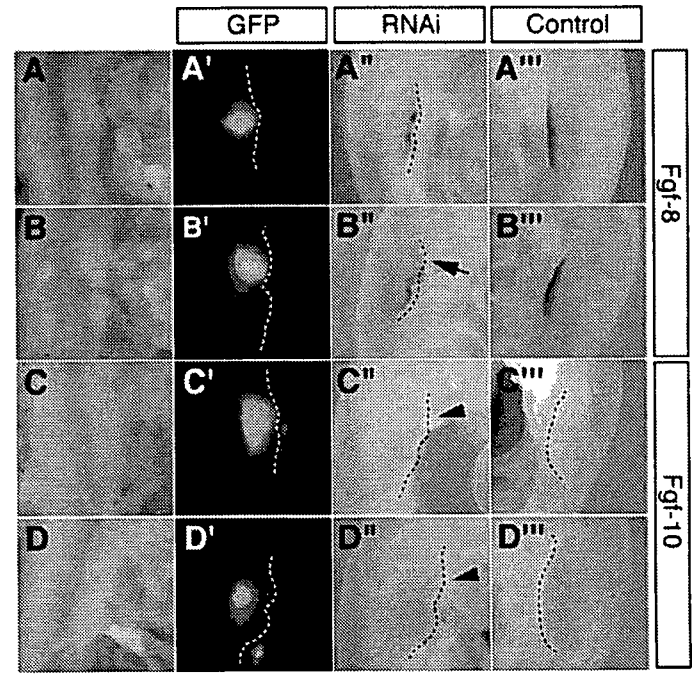

FIGURE 5. **HS2ST RNAi disrupted the FGF signaling loop.** *A–D*, *Fgf-8* and *Fgf-10* expression patterns at stage 18 (*A–C*) or 19 (*D*) were detected by whole-mount *in situ* hybridization (13–15 h after treatment). *A'–D'*, GFP signals, which were derived from coelectroporated pEGFP-N1, indicated the siRNA-injected region. *A''–D''*, right wing buds injected with 450 ng/μl esiRNA. *A'''–D'''*, the corresponding untreated left buds. *Fgf-8* expression in the ectoderm was significantly reduced by HS2ST RNAi treatment (*A* and *B*) and disappeared in the most affected regions (*arrow* in *B*). Similar to *Fgf-8* expression, *Fgf-10* expression in the mesoderm was also reduced in affected limbs (*arrowheads* in *C* and *D*).

luciferase esiRNA-injected buds (Fig. 6, *A* and *B*, *Group 3*). Interestingly in HS2ST esiRNA-injected but almost normally developed buds, increases of pERK and pAkt were also observed but not to the extent as those in Group 1 (about 1.5-fold) (Fig. 6, *A* and *B*, *Group 2*). When limb buds were sectioned and stained with anti-pERK antibody, a higher level of pERK was observed around the HS2ST esiRNA-injected region (Fig. 6*C*). These results suggest that phosphorylation of ERK and Akt was up-regulated by HS2ST RNAi, and truncation may be caused by up-regulation of these signaling molecules.

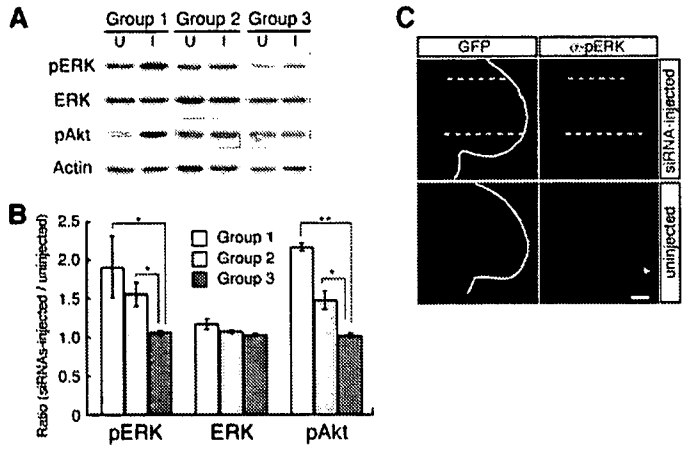

FIGURE 6. **Changes in ERK and Akt phosphorylation by HS2ST RNAi.** Phosphorylation of ERK and Akt was determined by Western blot analysis. *Group 1*, HS2ST esiRNA-injected and truncated limb buds (450 ng/μl). *Group 2*, HS2ST esiRNA-injected and almost normally developed limb buds (450 ng/μl). *Group 3*, luciferase esiRNA-injected and almost normally developed limb buds (300 ng/μl). *A*, Western blot analysis. Proteins were extracted from injected right buds (*I*) and the corresponding untreated left buds (*U*) of embryos at stage 23. *B*, the ratio of esiRNA-injected right buds to uninjected left buds. Each ratio of pERK, ERK, or pAkt is normalized to the respective actin expression. *Error bars* represent S.D. *, $p < 0.05$; **, $p < 0.01$ (Student's *t* test). *C*, localization of pERK. HS2ST siRNA-injected right bud and uninjected left bud at stage 23 were longitudinally sectioned and immunostained with anti-pERK antibody. A higher level of pERK was observed in AER (*arrowheads*) and ectoderm as reported previously (45). A relatively high level of pERK was observed in the HS2ST siRNA-injected region indicated by GFP signal (area between *dotted lines*), whereas a lower level of pERK was observed in the mesenchyme of uninjected control buds. *Scale bar*, 200 μm.

Alteration of HS Structures for FGF·FGFR Binding by HS2ST RNAi—FGF signaling was up-regulated by HS2ST RNAi. Thus, the complex formation of HS, FGF, and FGFR would be inevitably affected due to the alteration of the HS structure. To test this possibility, we subjected limb buds with or without the HS2ST RNAi treatment to ligand and carbohydrate engagement assays using FGF-8, FGF-10, and their specific receptors FGFR2c and FGFR2b. Limb bud sections were incubated with a mixture of FGF-8 and FGFR2c or FGF-10 and FGFR2b. We observed significantly strong binding of FGF-8 and FGFR2c to limb mesenchyme and weak binding to basement membranes and ectoderm including the AER (Fig. 7*A*). No binding was detected without FGFs or with the treatment with a mixture of heparitinases (Fig. 7*A*). In the HS2ST RNAi-affected region, the binding of FGF-8 and FGFR2c was significantly weak (Fig. 7*B*). On the other hand, we observed strong binding of FGF-10 and FGFR2b in the limb mesenchyme and basement membranes and weak binding in the ectoderm including the AER (Fig. 7*A*). In the RNAi-affected region, interestingly the binding of FGF-10 and FGFR2b was increased (Fig. 7*B*). The binding was particularly increased in the mesenchyme under the ectoderm (Fig. 7*B*). These results suggest that the reduction of 2-*O*-sulfate by RNAi changes HS structures in the limb bud in that FGF-10·FGFR2b had a tendency to bind more and FGF-8·FGFR2c had a tendency to bind less to HS in the mesenchyme. Considering effects on the *Fgf-8* and *Fgf-10* expressions observed in the RNAi-treated limb bud, these changes might affect the chick limb bud development.

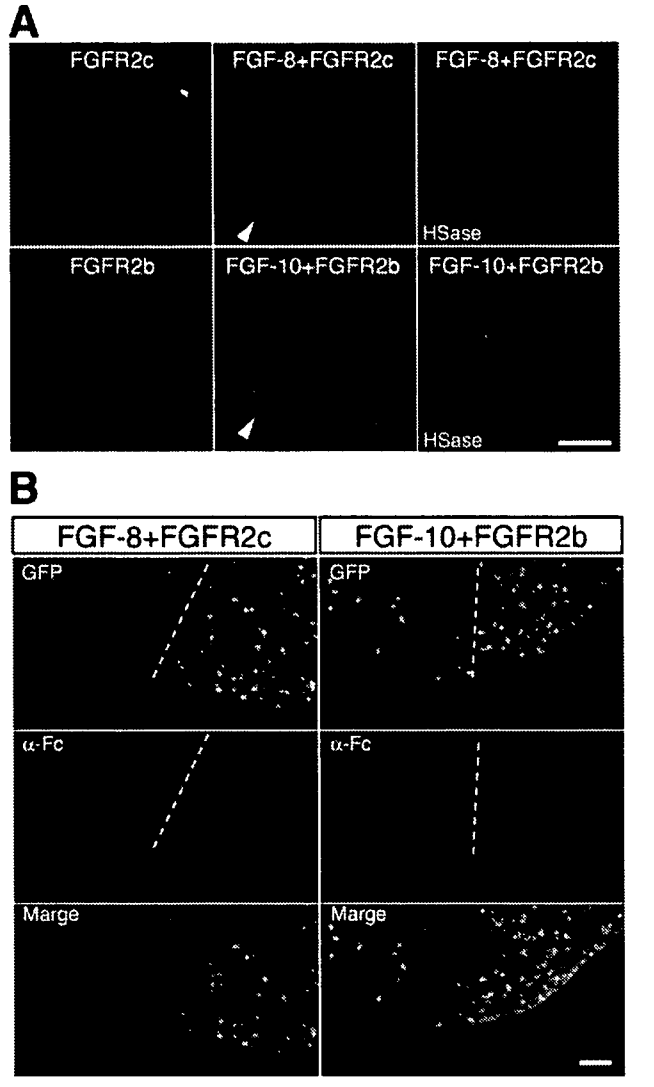

FIGURE 7. **Alteration of FGF and FGFR binding by HS2ST RNAi.** Interaction of FGF-8·FGFR2c and FGF-10·FGFR2b with HS was examined using the ligand and carbohydrate engagement assay. *A*, bindings of FGF-8·FGFR2c and FGF-10·FGFR2b on normal limb bud sections. Transverse sections of stage 23 limb buds were exposed to exogenous FGF-8 or FGF-10 and FGFR2c-Fc or FGFR2b-Fc and then probed with anti-Fc antibody. The binding of FGF-8·FGFR2c or FGF-10·FGFR2b was observed, whereas the binding of only FGFR2b or FGFR2c was not observed. When sections were pretreated with heparitinase (*HSase*), the bindings of FGF·FGFR were significantly reduced. Strong signals in the AER (*arrowheads*) were not detected either for the binding of FGF-8·FGFR2c or for that of FGF-10·FGFR2c. *Scale bar*, 50 μm. *B*, bindings of FGF-8·FGFR2c and FGF-10·FGFR2b in the longitudinal sections of limb bud after HS2ST RNAi treatment. GFP signals show RNAi-affected region. HS2ST siRNAs were injected into the area to the *right* of the *dotted lines*. The binding of FGF-10·FGFR2b is significantly increased in the RNAi-affected region, whereas the binding of FGF-8·FGFR2c is reduced in the RNAi-affected region. The nonspecific binding of FGF-8·FGFR2c was observed in the AER possibly due to the folding section. *Scale bar*, 50 μm.

DISCUSSION

Limb bud development is regulated by various growth factors, especially FGF-8 and FGF-10. HS is known to be involved in their signaling by its binding activity with specific structures (23). We therefore expected that the interaction between HS and growth factors requires a specific *O*-sulfation pattern. The expression patterns of HS *O*-sulfotransferases (HS2ST and HS6ST) are spatiotemporally regulated during embryogenesis and in adult tissues (34, 47, 48) and appear to coordinate with

changes in the activity of growth factors. To test this hypothesis, we examined the function of HS2ST in chick limb bud development. Inhibition of HS2ST (using siRNA mixtures) led to abnormal limb development and a disruption of AER formation and maintenance. This study provides the first evidence that HS2ST is essential for limb bud development.

Abnormal Limb Development by HS2ST RNAi—The knockdown of HS2ST in chick limb buds led to limb truncation, and the AER of these truncated limb buds did not function properly due to reduced *Fgf-8* expression (Figs. 4 and 5). *Fgf-8* expression in the prospective wing bud ectoderm begins in stage 16, and wing buds start to develop and grow in stage 17 (43). The activation of genes expressed in the AER, including *Fgf-8*, requires the signaling of FGF-10 derived from underlying mesenchymal cells. In the prospective forelimb region, *Fgf-10* is expressed in the LPM at stage 14-15 (5). In this study, we injected HS2ST siRNA mixtures into the LPM of the prospective forelimb region at stage 13-14. Although it is unknown how long it takes for RNAi-affected cells to completely replace normal HS with low 2-*O*-sulfated HS, the induction of *Fgf-10* expression in the LPM remains for several hours after RNAi treatment because it takes time to silence target genes and replace normal HS with *de novo* synthesized abnormal HS. Considering these factors, limb bud truncation by HS2ST knockdown occurs after AER induction by FGF-10. In fact, *Fgf-8* expression in the AER did not completely disappear after RNAi treatment (Figs. 4 and 5). Therefore, truncation by HS2ST RNAi is likely caused by the disruption of AER maintenance, which involves the FGF-8 and FGF-10 signaling loop and other factors such as Shh.

Role of 2-O-Sulfation in FGF Signaling Loop during Limb Development—Previous *in vitro* studies revealed that both 2-*O*-sulfation and 6-*O*-sulfation are necessary for FGF-8 to bind to HS, whereas only 6-*O*-sulfation is required for FGF-10 to bind to HS (23). Thus, a loss of 2-*O*-sulfation should not affect the binding of FGF-10 but should affect the binding of FGF-8. Bindings of FGF·FGFRs to HS may be different from bindings of FGFs to HS. In fact, interaction of FGF-8b and FGFR3c with HS was not affected in *Hs2st*-deficient mice, although interactions between FGF-8b and FGFR2c were not detected in the deficient mice (41). In the developing limb bud, FGFR2b and FGFR2c, which are specific to FGF-10 and -8, respectively, are expressed in the ectoderm and mesoderm, respectively (5, 6). Therefore, the suppression of 2-*O*-sulfation may interrupt FGF-8 signaling via FGFR2c in the mesoderm. Consistent with this estimation, a significant decrease in the FGF-8·FGFR2c binding was observed at the HS2ST RNAi-affected region (Fig. 7). The reason why the binding was still observed at the RNAi-affected region may be attributed to the remaining 2-*O*-sulfate residues because of incomplete loss of 2-*O*-sulfate residues by RNAi. In contrast, interaction of FGF-10·FGFR2b was significantly enhanced in the HS2ST RNAi-treated limb mesenchyme (Fig. 7*B*). Because FGFR2b is not expressed in the mesenchyme (5, 6), this result may explain the disruption of FGF-10 signaling as follows. FGF-10 is expressed in the limb mesenchyme and acts as a ligand in the AER, which expresses FGFR2b. Therefore, FGF-10 must diffuse to the AER from mesenchyme for signaling. HS in the HS2ST RNAi-treated mesenchyme would have a high affinity for FGF-10, and so FGF-10 in the treated mesenchyme might be difficult to diffuse to the AER and tend to remain in the mesenchyme. Furthermore in HS2ST mutant mice or HS2ST mutant *Drosophila*, a compensating increase in 6-*O*-sulfation has been observed (49, 50). If this is also the case with HS2ST knockdown limb buds, such highly 6-*O*-sulfated HS would bind more strongly to FGF-10 than would normal HS, resulting in the disruption of FGF-10 diffusion through the extracellular matrix.

Up-regulation of ERK and Akt Phosphorylation in HS2ST RNAi-treated Limb Buds—As the affected limb buds by HS2ST RNAi reduced *Fgf-8* and *-10* expressions and also possibly showed the interruption of FGF-8 and FGF-10 signaling as discussed above, it is likely that the signal transduction of FGFs may also be decreased. The reduction of *O*-sulfation is expected to decrease the phosphorylation of ERK under FGF signal transduction. For example, RNAi of *Drosophila* HS6ST reduces ERK phosphorylation in the tracheal system (33). However, we observed the up-regulation of ERK and Akt phosphorylation by HS2ST RNAi in developing limb buds (Fig. 6). This up-regulation of ERK and Akt phosphorylation could be caused by abnormal FGF signaling and other signaling through any tyrosine kinase receptors, although the respective mechanisms are estimated to be different. A more probable possibility is that the reduction of 2-*O*-sulfate affected the distribution or translocation of those HBGFs. The reduction of HS often causes the broad diffusion of HBGFs (9–11). Such abnormal distributions of HBGFs would widely activate their signals compared with localized HBGFs. In addition, fibroblast cells from HS2ST-deficient mice have a normal response for FGF-2 signaling although they have 2-*O*-sulfate-deficient HS that does not have binding activity with FGF-2 (49). Thus, the reduction of 2-*O*-sulfate in chick limb buds may affect the localization of HBGFs but not their signaling, although their signal levels and locations are probably imprecise, resulting in the up-regulation of pERK and pAkt.

Alternatively 2-*O*-sulfate of HS may negatively regulate the FGF signaling in chick limb bud development. In some reports, heavily 2-*O*-sulafted regions of HS are negative regulators of FGF signaling (51–54). If the 2-*O*-sulfation level in the limb bud is high enough to inhibit FGF signaling, HS2ST RNAi would reduce the inhibitory HS domain, resulting in the acceleration of FGF signaling. Because the interaction of FGF-8·FGFR2c was shown to decrease in the mesenchyme after RNAi, other FGF or FGFR signaling such as FGF-4 or FGFR1 may be up-regulated.

In chick limb bud development, both the MAPK/ERK and phosphatidylinositol 3-OH-kinase/Akt pathways have been shown to be essential for limb bud development and patterning (44–46). The ERK phosphorylation level in the limb bud is regulated by MAPK phosphatase 3, which antagonizes ERK phosphorylation and is induced through the phosphatidylinositol 3-OH-kinase/Akt pathway (45, 46). Recent reports have demonstrated that the MAPK/ERK pathway itself also induces MAPK phosphatase 3 expression and negatively regulates its phosphorylation level (pERK) in chick limb buds (46, 55). Indeed the levels of pERK and pAkt seemed to differ depending upon the different phenotypes or injections (Fig. 6*C*).

Application of FGF-8 or other FGF in the developing limb bud causes truncation, although such FGFs induce ectopic limb

buds in the flank of chick embryos (56, 57). In addition, it has been shown that ERK activation induces apoptosis in the limb mesenchyme (45). However, there has been no report on roles of Akt signaling in apoptosis during limb bud development, and this signaling is rather considered to have an antiapoptotic function (58). As it is possible that pERK and pAkt were up-regulated in different cells, abnormal apoptosis might happen to the cells with up-regulated pERK. Thus, knockdown of HS2ST by RNAi in the chick limb buds would cause abnormal apoptosis by up-regulation of ERK phosphorylation due to abnormal HS structures, resulting in truncation in severely affected limbs.

The Function of HS in Limb Development—We have shown that HS2ST is essential for wing bud development in chicken embryos. Interestingly the role of HS in limb bud development is different among tetrapods. In zebrafish, EXT2 and EXTL3 mutants resemble *Fgf-10* mutants, which have dysfunctional pectoral fins, suggesting that EXT2 and EXTL3 are required for FGF-10 signaling during fin bud development (59). Although the EXT family of genes are glycosyltransferases, which are responsible for HS chain synthesis, a similar fin bud defect also resulted from HS6ST knockdown in zebrafish (31). These reports indicate that fine structures of HS are essential for pectoral fin bud development in zebrafish. On the other hand, EXT1- or EXT2-deficient mice failed in gastrulation (60, 61). However, the hypomorphic mutation of EXT1 in mice resulted in reduced skeletal size, fusions of the elbow and knee joints, and occasionally syndactyly of digits (62). Similarly HS2ST or C-5 epimerase knock-out mice have a high frequency of polydactyly (28, 63). Considering these different effects depending upon the animal species, the fine structures of HS are more important being definitively involved in chick limb and fish fin development than in mammalian limb development. In fact, HS6ST expressions in developing limb reveal different patterns in these animals. For example, HS6ST-1 and -2 are expressed in AER of developing mouse limb bud, whereas significant expressions of HS6STs in AER are not observed in chick limb and zebrafish fin (34, 48, 64). Thus, the different fine structures of HS may play different roles in the regulation of various growth factors and morphogen signaling, the extent of which appears to vary depending on different vertebrates.

In accordance with different expression patterns of HS modification enzymes, the expression of some Wnt family proteins in developing limb buds appears to be different between chicks and mice (65, 66). At the initiation stage of chick limb buds, Wnt2b is expressed in intermediate mesoderm and LPM in the prospective forelimb region, and Wnt8c is expressed in LPM at the prospective hind limb (67). Both signals induce and maintain the expression of *Fgf-10* and are capable of inducing ectopic limbs in the embryonic flank. However, similar expression patterns of Wnt2b and Wnt8c at the limb initiation stage were not detected in mouse embryos (68). FGF-10 induces Wnt3a expression in the AER of chick limb buds, leading to the induction of *Fgf-8* expression (69). In contrast, Wnt3, but not Wnt3a, is expressed ubiquitously in the mouse limb ectoderm (70). A conditional Wnt3 mutant mouse exhibits a lack of *Fgf-8* expression in the limb buds (71). Several recent studies show that heparan sulfate proteoglycans regulate Wnt/Wg signaling during vertebrate and invertebrate development (10, 72). Although it has not been shown whether specific HS structures are required for the interaction of Wnt family proteins, knockdown of zebrafish HS6ST caused the up-regulation of Wnt and hedgehog signaling (31). Similar up-regulation of Wnt signaling was demonstrated by the action of HS-specific 6-*O*-endosulfatases (73, 74). The up-regulation of this signaling is considered a result of the release of growth factors from HS by the reduction of 6-*O*-sulfation. It is likely that HS2ST RNAi affects specific Wnt signaling by a similar action. However, further studies are required to show such possibilities.

Acknowledgments—We thank N. Nagai, S. Ashikari-Hada, and K. Kamimura for technical support and helpful discussions.

REFERENCES

1. Martin, G. R. (1998) *Genes Dev.* **12,** 1571–1586
2. Niswander, L. (2003) *Nat. Rev. Genet.* **4,** 133–143
3. Tickle, C., and Münsterberg, A. (2001) *Curr. Opin. Genet. Dev.* **11,** 476–481
4. Tickle, C. (2003) *Dev. Cell* **4,** 449–458
5. Ohuchi, H., Nakagawa, T., Yamamoto, A., Araga, A., Ohata, T., Ishimaru, Y., Yoshioka, H., Kuwana, T., Nohno, T., Yamasaki, M., Itoh, N., and Noji, S. (1997) *Development* **124,** 2235–2244
6. Xu, X., Weinstein, M., Li, C., and Deng, C. (1999) *Cell Tissue Res.* **296,** 33–43
7. Lewandoski, M., Sun, X., and Martin, G. R. (2000) *Nat. Genet.* **26,** 460–463
8. Moon, A. M., and Capecchi, M. R. (2000) *Nat. Genet.* **26,** 455–459
9. Esko, J. D., and Selleck, S. B. (2002) *Annu. Rev. Biochem.* **71,** 435–471
10. Lin, X. (2004) *Development* **131,** 6009–6021
11. Häcker, U., Nybakken, K., and Perrimon, N. (2005) *Nat. Rev. Mol. Cell. Biol.* **6,** 530–541
12. Dealy, C. N., Seghatoleslami, M. R., Ferrari, D., and Kosher, R. A. (1997) *Dev. Biol.* **184,** 343–350
13. Niu, S., Antin, P. B., Akimoto, K., and Morkin, E. (1996) *Dev. Dyn.* **207,** 25–34
14. Paine-Saunders, S., Viviano, B. L., Zupicich, J., Skarnes, W. C., and Saunders, S. (2000) *Dev. Biol.* **225,** 179–187
15. Sherman, L., Wainwright, D., Ponta, H., and Herrlich, P. (1998) *Genes Dev.* **12,** 1058–1071
16. Schlessinger, J., Plotnikov, A. N., Ibrahimi, O. A., Eliseenkova, A. V., Yeh, B. K., Yayon, A., Linhardt, R. J., and Mohammadi, M. (2000) *Mol. Cell* **6,** 743–750
17. Pellegrini, L., Burke, D. F., von Delft, F., Mulloy, B., and Blundell, T. L. (2000) *Nature* **407,** 1029–1034
18. Allen, B. L., Filla, M. S., and Rapraeger, A. C. (2001) *J. Cell Biol.* **155,** 845–858
19. Nakato, H., and Kimata, K. (2002) *Biochim. Biophys. Acta* **1573,** 312–318
20. Habuchi, H., Habuchi, O., and Kimata, K. (2004) *Glycoconj. J.* **21,** 47–52
21. Habuchi, H., Suzuki, S., Saito, T., Tamura, T., Harada, T., Yoshida, K., and Kimata, K. (1992) *Biochem. J.* **285,** 805–813
22. Loo, B. M., and Salmivirta, M. (2002) *J. Biol. Chem.* **277,** 32616–32623
23. Ashikari-Hada, S., Habuchi, H., Kariya, Y., Itoh, N., Reddi, A. H., and Kimata, K. (2004) *J. Biol. Chem.* **279,** 12346–12354
24. Zak, B. M., Crawford, B. E., and Esko, J. D. (2002) *Biochim. Biophys. Acta* **1573,** 346–355
25. Grobe, K., Ledin, J., Ringvall, M., Holmborn, K., Forsberg, E., Esko, J. D., and Kjellén, L. (2002) *Biochim. Biophys. Acta* **1573,** 209–215
26. Habuchi, O. (2000) *Biochim. Biophys. Acta* **1474,** 115–127
27. Rosenberg, R. D., Shworak, N. W., Liu, J., Schwartz, J. J., and Zhang, L. (1997) *J. Clin. Investig.* **99,** 2062–2070
28. Bullock, S. L., Fletcher, J. M., Beddington, R. S., and Wilson, V. A. (1998) *Genes Dev.* **12,** 1894–1906
29. Habuchi, H., Nagai, N., Sugaya, N., Atsumi, F., Stevens, R. L., and Kimata, K. (2007) *J. Biol. Chem.* **282,** 15578–15588

30. Pratt, T., Conway, C. D., Tian, N. M., Price, D. J., and Mason, J. O. (2006) *J. Neurosci.* **26,** 6911–6923
31. Bink, R. J., Habuchi, H., Lele, Z., Dolk, E., Joore, J., Rauch, G. J., Geisler, R., Wilson, S. W., den Hertog, J., Kimata, K., and Zivkovic, D. (2003) *J. Biol. Chem.* **278,** 31118–31127
32. Chen, E., Stringer, S. E., Rusch, M. A., Selleck, S. B., and Ekker, S. C. (2005) *Dev. Biol.* **284,** 364–376
33. Kamimura, K., Fujise, M., Villa, F., Izumi, S., Habuchi, H., Kimata, K., and Nakato, H. (2001) *J. Biol. Chem.* **276,** 17014–17021
34. Nogami, K., Suzuki, H., Habuchi, H., Ishiguro, N., Iwata, H., and Kimata, K. (2004) *J. Biol. Chem.* **279,** 8219–8229
35. Pekarik, V., Bourikas, D., Miglino, N., Joset, P., Preiswerk, S., and Stoeckli, E. T. (2003) *Nat. Biotechnol.* **21,** 93–96
36. Hamburger, V., and Hamilton, H. L. (1951) *J. Morphol.* **88,** 49–92
37. Tamura, K., Amano, T., Satoh, T., Saito, D., Yonei-Tamura, S., and Yajima, H. (2003) *Mech. Dev.* **120,** 199–209
38. Yonei, S., Tamura, K., Ohsugi, K., and Ide, H. (1995) *Dev. Biol.* **170,** 542–552
39. Yonei-Tamura, S., Endo, T., Yajima, H., Ohuchi, H., Ide, H., and Tamura, K. (1999) *Dev. Biol.* **211,** 133–143
40. Morita, H., Shinzato, T., David, G., Mizutani, A., Habuchi, H., Fujita, Y., Ito, M., Asai, J., Maeda, K., and Kimata, K. (1994) *Lab. Investig.* **71,** 528–535
41. Allen, B. L., and Rapraeger, A. C. (2003) *J. Cell Biol.* **163,** 637–648
42. Pan, Y., Woodbury, A., Esko, J. D., Grobe, K., and Zhang, X. (2006) *Development* **133,** 4933–4944
43. Crossley, P. H., Minowada, G., MacArthur, C. A., and Martin, G. R. (1996) *Cell* **84,** 127–136
44. Corson, L. B., Yamanaka, Y., Lai, K. M., and Rossant, J. (2003) *Development* **130,** 4527–4537
45. Kawakami, Y., Rodríguez-León, J., Koth, C. M., Büscher, D., Itoh, T., Raya, A., Ng, J. K., Esteban, C. R., Takahashi, S., Henrique, D., Schwarz, M. F., Asahara, H., and Izpisúa Belmonte, J. C. (2003) *Nat. Cell Biol.* **5,** 513–519
46. Eblaghie, M. C., Lunn, J. S., Dickinson, R. J., Münsterberg, A. E., Sanz-Ezquerro, J. J., Farrell, E. R., Mathers, J., Keyse, S. M., Storey, K., and Tickle, C. (2003) *Curr. Biol.* **13,** 1009–1018
47. Habuchi, H., Tanaka, M., Habuchi, O., Yoshida, K., Suzuki, H., Ban, K., and Kimata, K. (2000) *J. Biol. Chem.* **275,** 2859–2868
48. Sedita, J., Izvolsky, K., and Cardoso, W. V. (2004) *Dev. Dyn.* **231,** 782–794
49. Merry, C. L., Bullock, S. L., Swan, D. C., Backen, A. C., Lyon, M., Beddington, R. S., Wilson, V. A., and Gallagher, J. T. (2001) *J. Biol. Chem.* **276,** 35429–35434
50. Kamimura, K., Koyama, T., Habuchi, H., Ueda, R., Masu, M., Kimata, K., and Nakato, H. (2006) *J. Cell Biol.* **174,** 773–778
51. Wilson, V. A., Gallagher, J. T., and Merry, C. L. (2002) *Glycoconj. J.* **19,** 347–354
52. Rahmoune, H., Chen, H. L., Gallagher, J. T., Rudland, P. S., and Fernig, D. G. (1998) *J. Biol. Chem.* **273,** 7303–7310
53. Guimond, S., Maccarana, M., Olwin, B. B., Lindahl, U., and Rapraeger, A. C. (1993) *J. Biol. Chem.* **268,** 23906–23914
54. Pye, D. A., Vivès, R. R., Hyde, P., and Gallagher, J. T. (2000) *Glycobiology* **10,** 1183–1192
55. Smith, T. G., Karlsson, M., Lunn, J. S., Eblaghie, M. C., Keenan, I. D., Farrell, E. R., Tickle, C., Storey, K. G., and Keyse, S. M. (2006) *FEBS Lett.* **580,** 4242–4245
56. Niswander, L., Tickle, C., Vogel, A., and Martin, G. (1994) *Mol. Reprod. Dev.* **39,** 83–89
57. Vogel, A., Rodriguez, C., and Izpisúa-Belmonte, J. C. (1996) *Development* **122,** 1737–1750
58. Cross, T. G., Scheel-Toellner, D., Henriquez, N. V., Deacon, E., Salmon, M., and Lord, J. M. (2000) *Exp. Cell Res.* **256,** 34–41
59. Norton, W. H., Ledin, J., Grandel, H., and Neumann, C. J. (2005) *Development* **132,** 4963–4973
60. Lin, X., Wei, G., Shi, Z., Dryer, L., Esko, J. D., Wells, D. E., and Matzuk, M. M. (2000) *Dev. Biol.* **224,** 299–311
61. Stickens, D., Zak, B. M., Rougier, N., Esko, J. D., and Werb, Z. (2005) *Development* **132,** 5055–5068
62. Koziel, L., Kunath, M., Kelly, O. G., and Vortkamp, A. (2004) *Dev. Cell* **6,** 801–813
63. Li, J. P., Gong, F., Hagner-McWhirter, A., Forsberg, E., Abrink, M., Kisilevsky, R., Zhang, X., and Lindahl, U. (2003) *J. Biol. Chem.* **278,** 28363–28366
64. Cadwallader, A. B., and Yost, H. J. (2006) *Dev. Dyn.* **235,** 3432–3437
65. Yang, Y. (2003) *Birth Defects Res. C Embryo Today* **69,** 305–317
66. Church, V. L., and Francis-West, P. (2002) *Int. J. Dev. Biol.* **46,** 927–936
67. Kawakami, Y., Capdevila, J., Büscher, D., Itoh, T., Rodríguez Esteban, C., and Izpisúa Belmonte, J. C. (2001) *Cell* **104,** 891–900
68. Agarwal, P., Wylie, J. N., Galceran, J., Arkhitko, O., Li, C., Deng, C., Grosschedl, R., and Bruneau, B. G. (2003) *Development* **130,** 623–633
69. Kengaku, M., Capdevila, J., Rodriguez-Esteban, C., De La Peña, J., Johnson, R. L., Belmonte, J. C., and Tabin, C. J. (1998) *Science* **280,** 1274–1277
70. Parr, B. A., Shea, M. J., Vassileva, G., and McMahon, A. P. (1993) *Development* **119,** 247–261
71. Barrow, J. R., Thomas, K. R., Boussadia-Zahui, O., Moore, R., Kemler, R., Capecchi, M. R., and McMahon, A. P. (2003) *Genes Dev.* **17,** 394–409
72. Topczewski, J., Sepich, D. S., Myers, D. C., Walker, C., Amores, A., Lele, Z., Hammerschmidt, M., Postlethwait, J., and Solnica-Krezel, L. (2001) *Dev. Cell* **1,** 251–264
73. Ai, X., Do, A. T., Lozynska, O., Kusche-Gullberg, M., Lindahl, U., and Emerson, C. P., Jr. (2003) *J. Cell Biol.* **162,** 341–351
74. Dhoot, G. K., Gustafsson, M. K., Ai, X., Sun, W., Standiford, D. M., and Emerson, C. P., Jr. (2001) *Science* **293,** 1663–1666